

Determination of Structural and Geometrical Parameters of the Kribi-Campo Sedimentary Sub-Basin Using Gravity Data

Kue Petou Rokis Malquaire^{1,2,3*}, Owona Angue Marie Louise Clotilde^{3,4}, Njingti Nfor^{3,4}, Ndougsa-Mbarga Théophile^{3,4}, Manguelle-Dicoum Eliezer⁵

¹National Institute of Cartography, Yaoundé, Cameroon

²School of Geosciences, China University of Petroleum, Qingdao, China

³Postgraduate School of Sciences, Technologies & Geosciences, University of Yaoundé I, Yaoundé, Cameroon

⁴Department of Physics, Advanced Teacher Training College, University of Yaoundé I, Yaoundé, Cameroon

⁵Department of Physics, Faculty of Science, University of Yaoundé I, Yaoundé, Cameroon

Email: *rokis.petou@yahoo.fr

How to cite this paper: Malquaire, K.P.R., Clotilde, O.A.M.L., Nfor, N., Théophile, N.M. and Eliezer, M.D. (2017) Determination of Structural and Geometrical Parameters of the Kribi-Campo Sedimentary Sub-Basin Using Gravity Data. *International Journal of Geosciences*, 8, 1210-1224. <https://doi.org/10.4236/ijg.2017.89069>

Received: August 11, 2017

Accepted: September 27, 2017

Published: September 30, 2017

Copyright © 2017 by authors and Scientific Research Publishing Inc.

This work is licensed under the Creative Commons Attribution International License (CC BY 4.0).

<http://creativecommons.org/licenses/by/4.0/>



Open Access

Abstract

In order to produce a more detailed structural and geometrical information, and determine sediments thickness along the Kribi-Campo sub-basin, statistical spectral analysis and horizontal gradient analysis of residual anomalies coupled with the Euler deconvolution approach were applied on the gravity data in the area. The results obtained from the 2D spectral analysis on anomaly grids gave a depth to the basement rocks of the basin from 0.60 km to 3.93 km. This represents the thickness of the sedimentary formations overlying the basement. The interpretation of the spectral analysis results indicated that the potential hydrocarbon field areas are situated between Kribi and Lolabe and at Campo given that those areas have the highest sedimentary thicknesses values. From the analysis of the horizontal gradient, deep faults mainly striking SW-NE have been traced and a structural map of the area has been produced. By applying the Euler deconvolution method to the gravity data, information about the depth and trend of the main subsurface structures have been obtained.

Keywords

Sediment Thickness, Spectral Analysis, Horizontal Gradient, Structural Map, Kribi-Campo Sub-Basin, Gravity Data

1. Introduction

The Kribi-Campo basin is located at the northern edge of the South Atlantic rift

and is one of a series of divergent passive margin basins along the west coast of Africa. Covering a total area of about $6.2 \times 10^3 \text{ km}^2$, it was formed during the Mesozoic to Tertiary, as a result of the rifting of Africa and South America during the break-up of the Gondwana supercontinent [1]. This basin lies in the South west coast of Cameroun. Abundant oil seeps exist at the basin margins and a number of oil and gas discoveries have been made so far. Many authors, using both gravity and magneto-telluric data, have published on the structure of the subsurface in the entire South Cameroon. One of the most pertinent geophysical studies done in the Kribi-Campo basin is the 3D modelling, using gravity data, of an anomalous body located in the northern part of the basin [2]. The model obtained suggested that the basin's subsurface is intruded by a massive dense block composed of gneiss and granodiorite which has a thickness of about 4.5 km. The authors also suggested that this high density intrusive body is surrounded by sediments and metamorphic formations. [3] [4] also provided valuable information in the area by delineating some major discontinuities traversing the subsurface. In this paper, we are proposing the use of statistical spectral analysis, horizontal gradient and Euler deconvolution approaches to determine the structural and the geometrical characteristics (the majors and minor discontinuities, their trend and the thickness of the basin) in order to provide further interpretation of the Kribi-Campo basin subsurface structure and locate the areas with high sedimentary thicknesses which are potential targets in hydrocarbon exploration.

2. Geological and Tectonic Settings

The geological formations of Kribi in South Cameroon belong to four major lithological and structural units [5], the Ntem Archean unit; the Nyong Unit; the Neo-proterozoic cover and sedimentary formations. The study area is situated at northern edge of the Congo craton, at the transition zone between this mega-structure and the Mobile zone. The most relevant geological formations that can help to better describe this area are mainly the lower Nyong Unit formations and the sedimentary formations. The lower Nyong Unit is made up of ancient Archean rocks of the Ntem basement that underwent Eburnean orogenesis, their formation resulted from the collision between the Congo craton and the São Francisco [6] [7]. This unit was subject to high degree Tectonometamorphism dated $\pm 2050 \text{ Ma}$ associated to the charnokites formations dated $\pm 250 \text{ Ma}$ confirming the hypothesis that the Nyong Unit is a remobilized portion of the Archean Ntem complex [5]. The rocks in this area are mainly schists, gneisses that have been intruded by granodiorites and sedimentary formations rocks such as limestones and sandstone [8] [9].

In general, the region has a complex and uneven tectonic structure. This tectonic seems to have given rise to a vertical movement of the basement with subsidence to the North and uplift to the South [10] [11]. This basement movement must have provoked irregularities in the formations at depth, giving rise to faults, horsts and grabens characteristic of the boundary between the Congo Craton and the Pan-African folds belt [12]. The main faults in the region consist of the

Kribi-Campo Fault (KCF) system which is also considered as a continuation of the Sanaga Fault. This fault system is linked to the offshore fault system called the Kribi Fracture Zone. Contacts and faults trending E-W, N-S, NE-SW and NW-SE, which are either deep and/or buried structures and circular features which correspond to contacts and intrusive bodies have also been highlighted and characterized in the region [2] [4].

3. Material and Methods

3.1. Data Used

Two datasets have been combined to carry out this work: the existing ORSTOM data and the newly collected ones. In **Figure 2**, we present the distribution of the gravity data alongside with the altitude variation in the study area. The ORSTOM data (collected during the ORSTOM survey in 1968) [13] represented by red triangles have been combined with the new gravity data (collected by the team of geophysicist of the University of Yaoundé 1 in March 2015) represented by the blue squares. The new data constitute over 223 points measured along the basin area with a spacing of 0.5 to 1 km. These data were collected using the La-coste-Romberg G-823 gravity-meter. The irregularity in the data spacing is due to the inaccessibility of some sites given that the study area is found in the dense equatorial forest and the Campo National park where only open field roads are accessible.

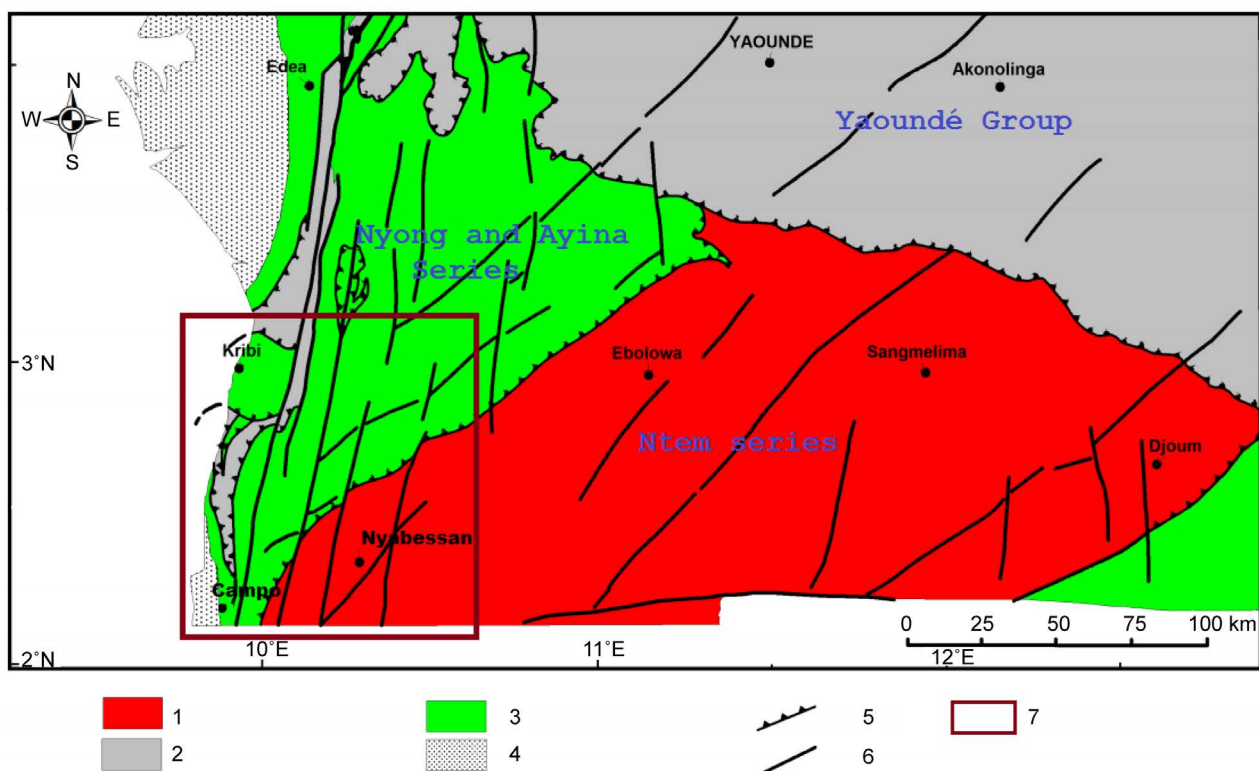


Figure 1. Simplified geological map of the SW-Cameroon [5]. 1: Archaean Basement; 2: Neoproterozoic cover; 3: Neoproterozoic-paleoproterozoic cover; 4: Post Panafrican cover; 5: Thrust fault; 6: fault; 7: Study area.

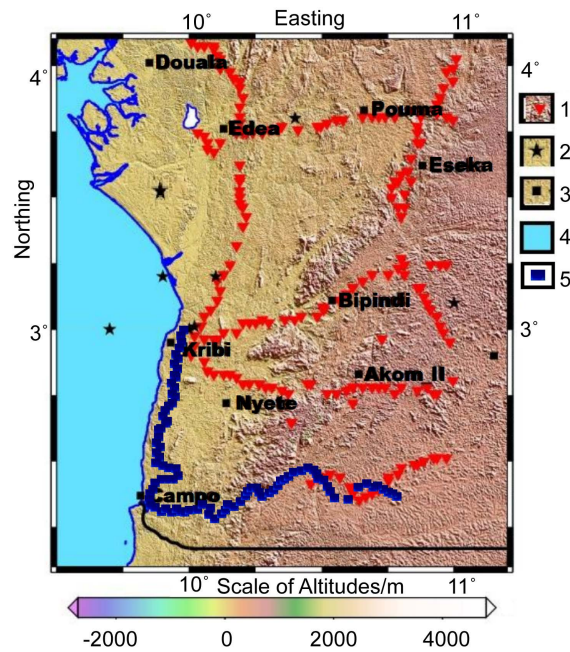


Figure 2. Gravity data distribution map showing the area with altitudes variations. 1: old data points, 2: earthquake epicenters, 3: localities, 4: sea, 5: new gravity data points (March 2015).

3.2. Spectral Analysis

This method is carried out through 2D Fast Fourier Transform which transforms gravity data from the space domain to the wavenumber domain to estimate the depths of the structures responsible for the measured anomaly. It has been used extensively by many authors, namely [14] [15] [16].

The finite discrete Fourier transform is given by the equation:

$$B(\omega) = \sum_0^{N-1} b(x) \exp(-i\omega x) \cdot \Delta x \quad (1)$$

where $b(x)$ represents the discrete N data array of gravity data obtained by sampling a continuous profile at evenly spaced intervals Δx . i is the complex operator, $\omega = 2\pi k$ is the spatial frequency and $k = \lambda^{-1}$ is the wavenumber in the x direction.

The expression of the Bouguer Slab Effect is then given by the equation:

$$B(k)_{z=0} = 2\pi\Delta\rho G \cdot \exp(-2\pi kt) \cdot F(k)_{z=0} \quad (2)$$

where $B(k)_{z=0}$ is the Fourier transform of the Bouguer anomaly profile $b(k)_{z=0}$; $\Delta\rho$ is the density contrast between two layers; $F(k)$ is the Fourier transform of $f(x)$, the derivation of the interface from the mean depth z ; G is the gravitational constant. The mean depth can then be calculated using the following equation:

$$h = \frac{\Delta \text{Log} E}{4\pi\Delta k} \quad (3)$$

where E is the power spectrum of $B(k)$.

When the square of the Fourier amplitude spectrum is plotted against the radial frequency, the slope of the relationship between the wave number of the gravity field and the logarithmic power spectrum provide information about the depths to basement of the anomaly sources.

3.3. Euler Deconvolution

The Euler Method is a technique generally used to locate the apparent depth to the gravity or magnetic anomaly source. Considering a degree of homogeneity, the gravity or magnetic field is related to its gradient component in order to trace the surface of the ground contact. The degree of homogeneity is expressed by the structural index which defines the measure of the fall-off rate of the field with distance from the source. The Euler homogeneity equation is given as:

$$(x - x_0) \frac{\partial T}{\partial x} + (y - y_0) \frac{\partial T}{\partial y} + (z - z_0) \frac{\partial T}{\partial z} = N(B - T) \quad (4)$$

where (x_0, y_0, z_0) is the position of the magnetic or gravity source whose total field (T) is detected at (x, y, z) . B is the regional gravity or magnetic field. N is the measure of the fall-off rate of the gravity field and may be interpreted as the structural index (SI). This value needs to be chosen according to a prior knowledge of the source geometry.

The Euler depth appear wherever there are lithological discontinuities in the geological formations. They represent the structural and/or stratigraphic changes of various geological formations [3].

3.4. The Horizontal Gradient Method

According to [17], the horizontal gradient performed at different heights of the anomaly observation allows for the location of discontinuities and the determination of their dip.

The horizontal gradient is an operation that measures the rate of change of a potential field in the x and y directions [18] in order to image subsurface structures. However, the total horizontal gradient magnitude (HGM) is preferred for its simplicity. The HGM operator is defined by the relation below:

$$HGM(x, y) = \sqrt{\left(\frac{\partial G}{\partial x}\right)^2 + \left(\frac{\partial G}{\partial y}\right)^2} \quad (5)$$

where G is the Bouguer gravity field.

The horizontal gradient method is used to locate the boundaries of density contrast from gravity data. These results mark the top edges of gravity or density boundaries. Thus, the maximum value of the horizontal gradient anomalies is placed on top of the sources edges. However, offsets occur when edges are not vertical or when several anomalies are close together. The biggest advantage of the horizontal gradient method is its low sensitivity to the noise in the data, be-

cause it only requires calculations of the two first-order horizontal derivatives (x - and y -directions) of the gravity field [4].

The works of [18] [19] showed that the maxima of the horizontal gradient of gravity anomalies help in locating contacts associated with abrupt changes in density, which are interpreted either as faults, geological contacts or intrusions. Faults are expressed by a quasi-linear disposition of at least three maxima and horizontal limits of intrusive bodies are shown by quasi-circular disposition of many maxima [20].

4. Results and Interpretation

4.1. Gravity Data Analysis

The gravity anomaly maps generally superpose the effects of deep, shallow, local and extended gravity contrasts. The effects of a local or shallow structure are often hidden in the signatures of regional structures. We carried out regional-residual separation using the polynomial fitting method with the aim of isolating the anomalies caused by deep and extended sources (long-wavelength anomalies) from those caused by local and shallow density contrasts (short wavelength anomalies). The residual field is obtained by estimating the regional gravity field and removing it from the observed field which is the Bouguer anomaly (**Figure 3**). In effect, the order of the regional field n is assimilated to a polynomial of n degree. When n is small, the regional anomaly possesses values which are relatively more different from those of the Bouguer anomaly. In this case, the thickness of the part of the crust causing the corresponding residual anomalies is relatively large. This thickness decreases when n increases. In fact,

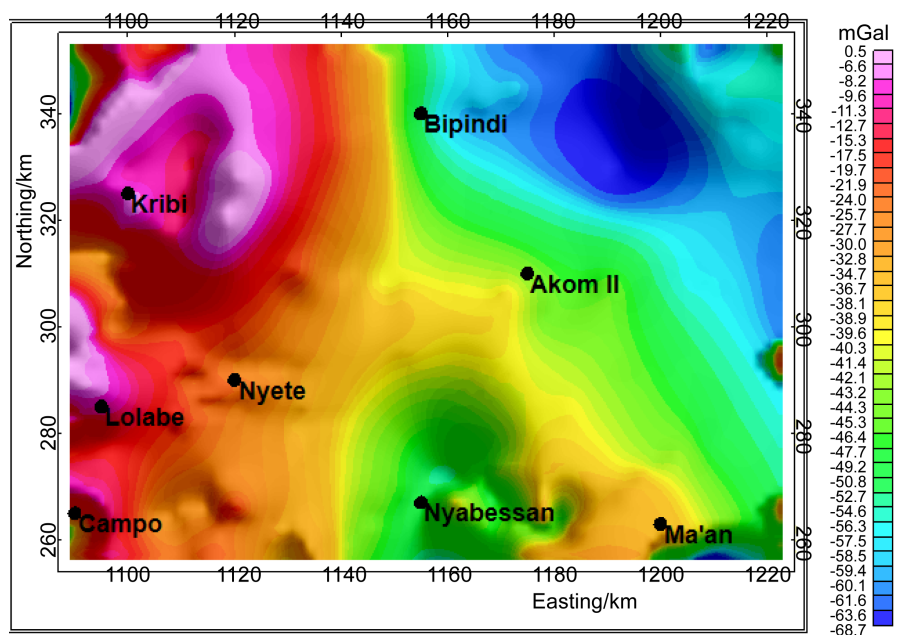


Figure 3. Bouguer anomaly map of the Kribi-Campo sedimentary sub-basin modified after [2].

the wavelength of the residual anomaly decreases when the degree of the polynomial increases thereby revealing geological structures which appear closest to the surface [20].

In this work, we have used a polynomial of degree '1', for spectral analysis, Horizontal gradient and Euler deconvolution, so as to have a better chance of locating the major contacts.

In **Figure 2**, we present the distribution of the gravity data alongside with the altitude variation in the study area. The ORSTOM data (collected during the ORSTOM survey in 1968) [21] represented by red triangles have been combined with the new gravity data (collected by the team of geophysicist of the University of Yaoundé 1 in March 2015) represented by the blue squares. The new data constitute over 223 points measured along the basin area with a spacing of from 0.5 km to 1.0 km. These data were collected using the Lacoste-Romberg G-823 gravity-meter. The irregularity in the data spacing is due to the inaccessibility of some sites given that the study area is found in the dense equatorial forest and the Campo National park where only open fields and roads are accessible.

In **Figure 3**, we present the Bouguer gravity anomalies. This map was obtained by interpolation of gravity data using the kriging gridding algorithm of the Oasis Montaj 8.0 software. As interpreted by [2], the Bouguer map of the area presents three gravity domains: the high gravity anomalies to the west, corresponding to a ring complex affected by a nearly N-S trending discontinuity and basic intrusive bodies within the main formation; the second domain to the north-east corresponding to low density intrusive bodies and the third domain in the middle of the map marking the signatures of charnockites and green rock belts of the Ntem Unit.

The first order residual map **Figure 4** reveals several local anomalies. The positive ones to the west at Kribi (A1), north-east of Kribi (A2), south-west of Kribi (A3), Lolabe (A4), Campo (A5) south-east of Lolabe (A6) and north of Kribi (A7) which indicate basement uplift and lateral differences in density from causative rocks. The Kribi positive anomaly is caused by an intrusive igneous body (gneiss, granodiorite) with a density estimated at about 2.74 g/cm^3 [2]. The Lolabe and Campo anomalies could also be the results of dense rocks intrusion oriented N-S and buried under the sedimentary cover. The main negative anomalies are observed in the northeast, central south and southeast parts of the study area trending NW-SE (A8), SW-NE at Nyabessan (A9) NW-SE (A10) at Ma'an and the nearly circular anomaly to the east of Bipindi (A11). [21] suggested that the nearly circular anomaly of Bipindi was caused by a low density intrusive block having a density contrast of -0.095 g/cm^3 .

4.2. Estimation of the Thickness of the Basin

We applied a 2D spectral analysis on grids centered on positive anomalies in the basin situated on the western area of the map (A1, A2, A3, A4, A5, A6, and A7), which enabled us to determine the depths. The power spectrum has been

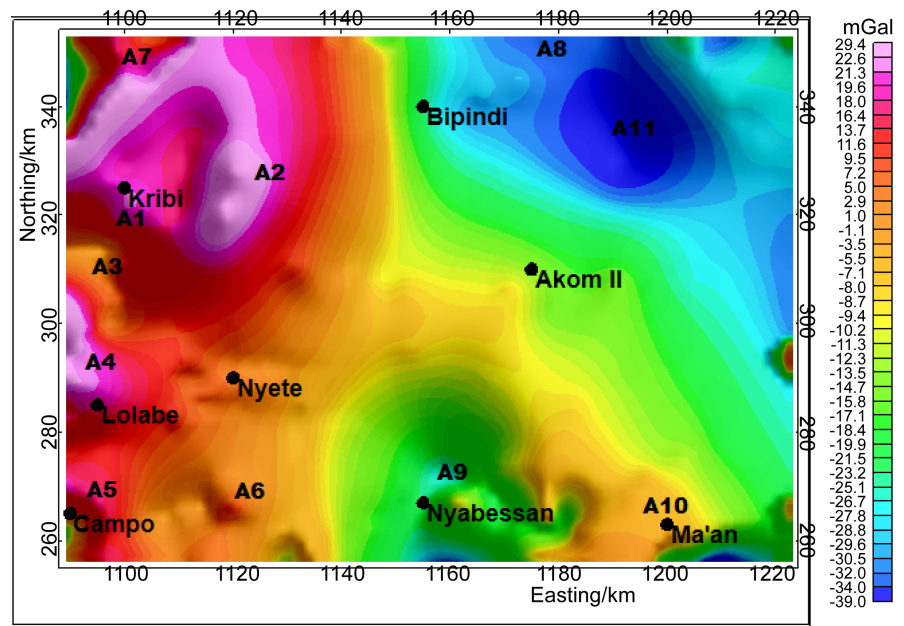


Figure 4. First order residual anomaly map of the study area.

obtained from the energy values which derive from the anomaly values. The given values are presented in **Table 1**.

Figure 5 presents a sample of the power spectrum curves obtained for the various anomaly grids. The line segment on this curve can be identified and plotted by a least squares fitting on the data points. This curve is obtained from the anomaly values of grid A2. The same calculation were carried out for A1, A3, A4, A5, A6 and A7. The mean depth of density contrast plane may be interpreted as an inter-basement density variation associated with the depth to basement [22]. This mean depth, highlighting the discontinuities observed for the positive anomalies has been calculated and presented in **Table 2**. The first observation that can be made from this table is that, the sedimentary infill thickness decreases as we move from the west to the east of the area. The depths to basement vary from 0.60 km to about 3.93 km. We also observe that there is a relatively high accumulation of sediments in the basin (>0.6 km). The areas with the highest depth to basement or highest sedimentary thickness (~4 km) are the most promising regions for oil and gas exploration. The zone situated between Kribi and Lolabe and the Campo area are well indicated for further prospections. These results are therefore important for the selection of new exploration areas.

4.3. Structural Parameters of the Basin

4.3.1. Horizontal Gradient Method

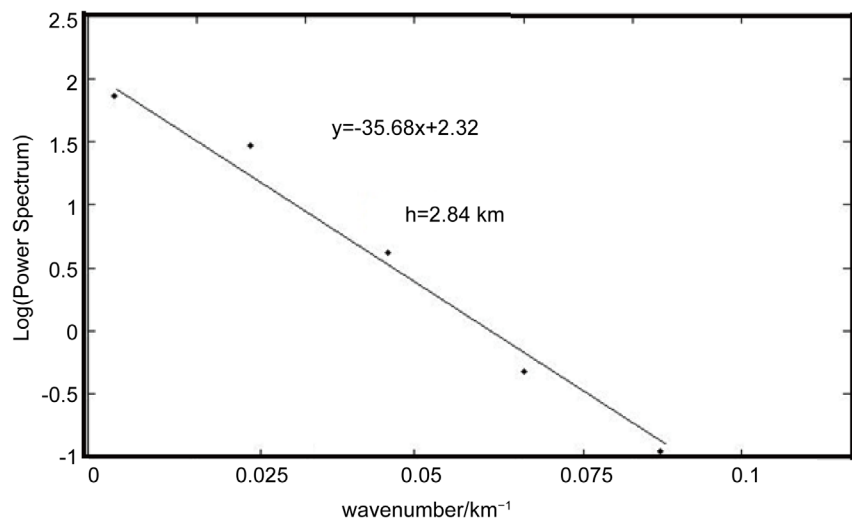
We used the Oasis montaj 8.0 software to calculate the amplitude of the horizontal gradient of the residual data of the study area (**Figure 6**). We can clearly observe on this map the regions with high gradient amplitude indicating high density variation between contacts. The two major lineament that are interpreted from this map are striking in the direction NW-SE from Kribi right

Table 1. Anomaly Values, Power Spectrum and wavenumber values for the anomaly grid A2.

ANOMALY VALUES/ mGal	POWER SPECTRUM	LOG (POWER SPECTRUM)	WAVENUMBER/ km ⁻¹
-50.00	87.44	1.95	0.02
-12.60	2.06	0.33	0.07
-4.19	0.40	-0.40	0.09
-7.58	0.11	-0.95	0.11
-9.22	0.04	-1.40	0.15

Table 2. Depths to basement obtained from power spectrum of gravity data.

ANOMALY ID	DEPTH TO BASEMENT/km
A1	2.62
A2	2.84
A3	3.48
A4	0.97
A5	3.93
A6	0.60
A7	1.19

**Figure 5.** Power spectrum of the gravity data. The linear segment correspond to the density layer used to compute depth.

to Nyabessan and from Lolabe to the south east of Campo. The east of Bipindi is also characterized by high gradient variation. This could mark the huge change in density between the Bipindi intrusive block and metamorphic formations surrounding it. Due to the broad nature of the high gradients, we suggest that the boundaries of density contacts in the Kribi-Campo basin are probably not

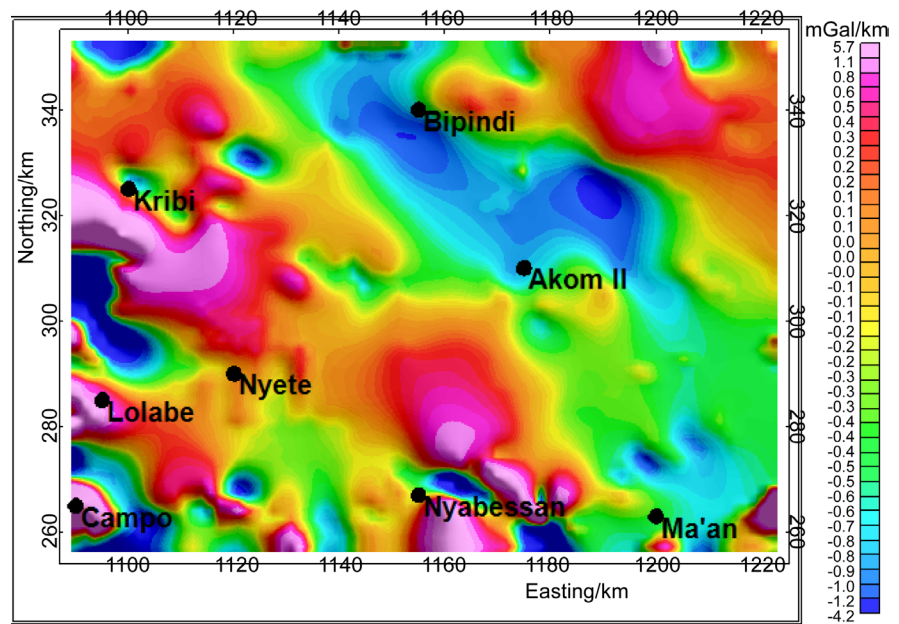


Figure 6. Horizontal gradient map of the study area.

necessarily vertical and relatively deep or produced by several boundaries.

4.3.2. Euler Solutions

For the Euler method, the following parameters have been used to compute the Euler solutions: structural Index $N = 0.5$, maximum % of tolerance of 5 and a window size of $5 \text{ km} \times 5 \text{ km}$. **Figure 7** shows the results of the Euler method from the first order residual gravity data. This map presents the structural layout of the area showing the different faults affecting the subsurface. The computed depths vary between 2.0 km and 20.4 km for the entire region and between 2.0 km and 7.0 km for the western zone which makes up the basin. It is observed that the faults and contacts highlighted here get deeper as we move to the east. The shallowest are those located in the basin area at the extreme west and in the extreme south zone of the map. We present in the first column of **Table 3** the various faults delineated using the Euler deconvolution approach, the orientations of these faults are given in the second column; it is observed that the SW-NE is the main fault direction in the basin. This information can be helpful in the determination of fluid flow direction in the basin. The last column of **Table 3** gives the depth range of faults, the shallowest identified from 2 km and the deepest at about 12 km of depth. The different faults detected in the basin area can be interpreted as a result of local tectonic movements coupled with the setting up of intrusive rocks (granodiorites and gneisses) into the sedimentary and metamorphic formations.

4.3.3. Structural Map of the Basin

The combination of the above described results, namely the spectral analysis, horizontal gradient and Euler solutions coupled with the results published by [2] have enabled us to propose a structural map of the Kribi-Campo sedimentary

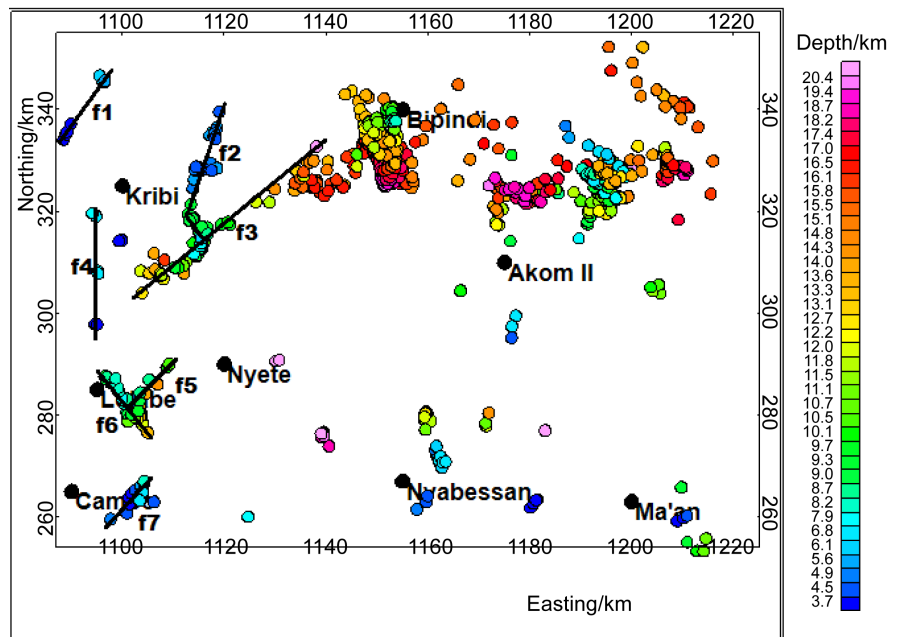


Figure 7. Structural interpretation of Euler Solutions for $N = 0.5$. The black lines represent the highlighted faults.

Table 3. Direction and Depth range of Faults in the Basin.

FAULT ID	DIRECTION	DEPTH RANGE/km
f1	SW-NE	2 - 5
f2	SSW-NNE	2 - 4
f3	SW-NE	7 - 13
f4	NS	2 - 5
f5	SW-NE	2 - 6
f6	NNW-SSE	6 - 12
f7	SW-NE	2 - 8

basin (**Figure 8**). This map shows quasi-linear contacts (numbered 1 to 12) which can describe faults and quasi-linear contacts (denoted C_1 , C_2 and C_3) corresponding to horizontal limits of intrusive bodies.

5. Discussion

The results presented in the above sections are in accordance with the fact that the Kribi-Campo basin formations are relatively shallow compared to the Douala and Garoua basins. The general disposition of anomalies on the first order residual anomaly map (**Figure 4**) shows a west-to east diminution in the anomaly values which indicates the same variation of density values. According to [2], the Kribi zone is intruded by a 4.5 km thick block of body composed of gneiss and granodiorites. This intrusion has considerably influenced the sedimentary cover in the area. From the results of the sedimentary thickness

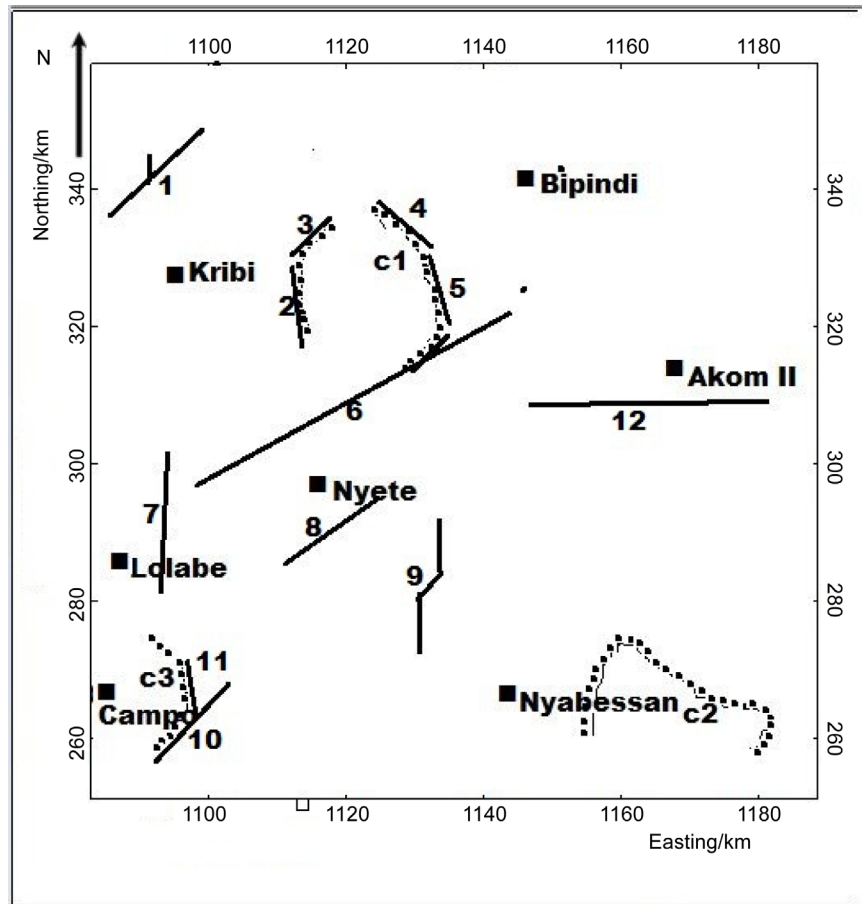


Figure 8. Interpreted structural Map of the Kribi Campo basin. (1) to (12): linear contacts; (C₁), (C₂) and (C₃): circular contacts indicating boundaries of intrusions.

obtained by spectral analysis, it can be seen that as we move from the North to the South of the study area, the sedimentary layer varies following a sinusoidal trend. This variation of the sediment thickness could be explained by the presence of high tectonic activities in the area [9] leading either to an uprising or to a subsidence of the basement. The smallest value of this thickness agrees with the works of [2] which proposed a 3D model of an intrusive body buried in a 0.5 km sediment layer. The horizontal gradient map shows that the boundaries of density contacts in the Kribi-Campo basin are not vertical and are relatively deep or produced by several boundaries because of the broad nature of the high gradients. From Figure 7 it has been shown that the discontinuities and contacts in the Kribi-Campo basin are relatively shallow. These contacts get deeper as we move into the continent. Seven (7) major faults have been delineated (from f1 to f7) each with its direction and depth range. The analysis of the structural map of the basin highlights the presence of: (1) contacts and faults trending mainly SW-NE, N-S, SSW-NNE and NNW-SSE which confirms the results of [3] [4] giving the same approximate directions to major lineaments in the region and (2) three circular contacts C₁, C₃ and C₃ representing rocks intrusions amongst which one had been characterized and modelled in the works of [2]. This study

also suggests that given the high sedimentary thickness, the area situated between Kribi and Lolabe and the Campo locality are of high potential in mining and/or hydrocarbon resources. This suggestion is supported by the fact that the presence of oil and gas in a basin might be due to two factors: in-situ generation and migration of fluids into the basin [22]. The subsurface pressure which is a function of the sediment thickness (*i.e.*, the sediment weight) is one of the environmental conditions needed for oil and gas formation in a basin. The understanding of the fluid flow formation in the region could be elucidated by Euler solutions, the structural map and gradient maps analysis.

6. Conclusion

The aim of this study was to provide new insights on the structural setting and the geometrical characteristics of the Kribi-Campo basin. We used the polynomial fitting method to carry out the separation of the residual and regional components of the gravity field. We observed that the positive residual anomalies in the area are the effect of both high density rocks intrusions and sedimentary infill. The spectral analysis enabled to estimate the depth to basement on various parts of the Kribi-Campo basin which gives the sedimentary thickness. This thickness varies from 0.60 km to 3.93 km with the highest values obtained in some specific localities of the study area namely Campo and the area between Kribi and Lolabe. From the residual anomaly map and spectral analysis it can be deduced that the sedimentary infill presents a discontinued north-south variation and also decreases from the west towards the east as we move from the coast into the continent. We applied the horizontal gradient analysis to the residual component. The residual structural setting of the zone from the Euler method is characterized by major faults and contacts mainly oriented SW-NE with the shallowest in the west (from 2 to 7 km deep) and the deepest in the east (right down to 20 km deep) of the region. The use of spectral analysis and Euler solutions is very advantageous in the geometrical and structural characterization of gravity anomalies in the sense that they help not just to determine depths to basement of causative structures but also to evaluate their dip and their evolution in the longitudinal and transversal directions. The structural map of the basin provides the most relevant structural information in the area. This map can help in identifying the direction of fluid flow in the subsurface. The interpretation of the sedimentary thickness values can serve to identify areas with the highest mineral and hydrocarbon production potentials which correspond to areas with the highest sedimentary thickness.

Acknowledgements

The authors are thankful to the University of Yaoundé 1 and the Ministry of Higher Education for funding the data acquisition campaign. All reviewers of this manuscript are equally acknowledged.

References

- [1] Perez-Diaz, L. and Eagles, G. (2014) Constraining South Atlantic Growth with Seafloor Spreading Data. *Tectonics*, **33**, 1848-1873.
<https://doi.org/10.1002/2014TC003644>
- [2] Kue Petou, R.M., Owona Angue, M.L., Njingti, N., and Manguelle-Dicoum, E. (2017) 3D Modelling from New and Existing Gravity Data of an Intrusive Body in the Northern Part of Kribi-Campo Sub-Basin in Cameroon. *International Journal of Geosciences*, **8**, 984-1003. <https://doi.org/10.4236/ijg.2017.88056>
- [3] Owona Angue, M.L.C., Tabod, C.T., Nguiya, S., Kenfack, J.V. and Tokam Kamga, A.P. (2013) Delineation of Lineaments in South Cameroon (Central Africa) Using Gravity Data. *Open Journal of Geology*, **3**, 331-339.
<https://doi.org/10.4236/ojg.2013.35038>
- [4] Owona Angue, M.L.C., Assembe, S.P., Njingti, N., Ngoh, J.D., Ndougsa Mbarga, T., Kue Petou, R.M. and Bisso, D. (2016) Determination of the Structural Lineaments in the Kribi-Campo-Ma'an Area from a Multi-Scale Analysis of Gravity Data Using the HGM and Euler 3D Deconvolution Approaches. *International Journal of Geosciences*, **7**, 1122-1143. <https://doi.org/10.4236/ijg.2016.79085>
- [5] Maurizot, P., Abessolo, A., Feybesse, J.L., Johan, V. and Lecomte, P. (1986) Etude et prospection minière du sud-ouest Cameroun. Synthèse des travaux de 1978 à 1985. [Study and Mining Prospecting of Southwestern Cameroon. Synthesis of the Work from 1978 to 1985.] Rapport, BRGM, 274 p.
- [6] Toteu, S.F., Van Schmus, R.W., Penaye, J. and Nyobe, J.B. (1994) U-Pb and Sm-Nd Evidence for Eburnian and Pan-African High-Grade Metamorphism in Cratonic Rocks of Southern Cameroon. *Precambrian Research*, **67**, 321-347.
- [7] Feybesse, J.L., Barbossa Ledru P., Guerrot, C., Johan, V., Triboulet, V., Bouchot, V., Prian, J.P. and Sabate, P. (1995) Paleoproterozoic Tectonic Regime and Markers of the Archean/Proterozoic Boundary in the Congo-Sao Francisco Craton EUG 8, Terra Abstracts P 100.
- [8] Toteu, S.F., Penaye, J. and Poudjom Djomani, Y.H. (2004) Geodynamic Evolution of the Pan-African Belt in Central Africa with Special Reference to Cameroon. *Canadian Journal of Earth Sciences*, **41**, 73-85. <https://doi.org/10.1139/e03-079>
- [9] Owona Angue, M.L.C., Nguiya, S., Nouayou, R., Tokam Kamga, A.P. and Manguelle-Dicoum, E. (2011) Geophysical Investigation of the Transition Zone between the Congo Craton and the Kribi-Campo Sedimentary Basin (South-West Cameroon). *South African Journal of Geology*, **114**, 145-158.
<https://doi.org/10.2113/gssajg.114.2.145>
- [10] Manguelle-Dicoum, E. (1988) Etude Géophysique des structures superficielles et profondes de la région de Mbalmayo. [Geophysical Study of the Superficial and Deep Structures of the Mbalmayo Region.] PhD Thesis, Université de Yaoundé I, Yaoundé, 202 p.
- [11] Shandini, Y. and Tadjou, J.M. (2012) Interpreting Gravity Anomalies in South Cameroon, Central Africa. *Earth Sciences Research Journal*, **16**, 5-9.
- [12] Shandini, N.Y., Tadjou, J.M., Tabod, C.T. and Fairhead, J.D. (2010) Gravity Data Interpretation in the Northern Edge of the Congo Craton, South-Cameroon. *Anuário do Instituto de Geociências*, **33**, 73-82.
- [13] Collignon, F. (1968) Gravimétrie et reconnaissance de la République Fédérale du Cameroun. [Gravimetry and Recognition of the Federal Republic of Cameroon.] ORSTOM, Paris, 35 p.
- [14] Spector, A. and Grant, F.S. (1970) Statistical Models for Interpretation Aeromag-

- netic Data. *Geophysics*, **35**, 293-302. <https://doi.org/10.1190/1.1440092>
- [15] Gerard, A. and Debeglia, N. (1975) Automatic Three-Dimensional Modeling for Interpretation of Gravity or Magnetic Anomalies. *Geophysics*, **40**, 1014-1034. <https://doi.org/10.1190/1.1440578>
- [16] Bhattacharyya, B.K. and Leu, L.-K. (1975) Spectral Analysis of Gravity and Magnetic Anomalies Due to Two-Dimensional Structures. *Geophysics*, **40**, 993-1013. <https://doi.org/10.1190/1.1440593>
- [17] Archibald, N.J., Gow, P. and Boschetti, F. (1999) Multiscale Edge Analysis of Potential Field Data Exploration. *Geophysics*, **30**, 38-44.
- [18] Cordell, L. and Grauch, V.J.S. (1985) Mapping Basement Magnetization Zones from Aeromagnetic Data in the San Juan Basin, New Mexico. In: Hinze, W.J., Ed., *The Utility of Regional Gravity and Magnetic Anomaly Maps*, Society of Exploration Geophysicists, 181-197. <https://doi.org/10.1190/1.0931830346.ch16>
- [19] Cordell, L. (1979) Gravimetric Expression of Graben Faulting in Santa Fe Country and the Espanola Basin, New Mexico. In: Ingersoll, R.V., Ed., *Guidebook to Santa Fe Country*, New Mexico Geological Society, Socorro, 59-64.
- [20] Koumetio, F., Njomo, D., Tabod, C.T., Noutchogwe, T.C. and Manguelle-Dicoum, E. (2012) Structural Interpretation of Gravity Anomalies from the Kribi-Edea Zone, South Cameroon: A Case Study. *Journal of Environmental & Engineering*, **9**, 664-673. <https://doi.org/10.1088/1742-2132/9/6/664>
- [21] Koumetio, F., Njomo, D., Tatchum, C.N., Tokam, K.A.P., Tabod, C.T. and Manguelle-Dicoum, E. (2014) Interpretation of Gravity Anomalies by Multi-Scale Evaluation of Maxima of Gradients and 3D Modelling in Bipindi Region (South-West Cameroon). *International Journal of Geosciences*, **5**, 1415-1425. <https://doi.org/10.4236/ijg.2014.512115>
- [22] Mouzong, M.P., Kamguia, J., Nguiya, S., Shandini, Y. and Manguelle-Dicoum, E. (2014) Geometrical and Structural Characterization of Garoua Sedimentary Basin, Benue Trough, North Cameroon, Using Gravity Data. *Journal of Biology and Earth Sciences*, **4**, 25-33.



Submit or recommend next manuscript to SCIRP and we will provide best service for you:

Accepting pre-submission inquiries through Email, Facebook, LinkedIn, Twitter, etc.
A wide selection of journals (inclusive of 9 subjects, more than 200 journals)
Providing 24-hour high-quality service
User-friendly online submission system
Fair and swift peer-review system
Efficient typesetting and proofreading procedure
Display of the result of downloads and visits, as well as the number of cited articles
Maximum dissemination of your research work

Submit your manuscript at: <http://papersubmission.scirp.org/>

Or contact ijg@scirp.org